JACS
JOURNAL OF THE AMERICAN CHEMICAL SOCIETY
Article
Cite This: J. Am. Chem. Soc. XXXX, XXX, XXX−XXX
pubs.acs.org/JACS

Independent Generation of Reactive Intermediates Leads to an Alternative Mechanism for Strand Damage Induced by Hole Transfer in Poly(dA−T) Sequences

Huabing Sun,[†] Liwei Zheng,[†] and Marc M. Greenberg*

Department of Chemistry, Johns Hopkins University, 3400 North Charles Street, Baltimore, Maryland 21218, United States

Supporting Information

ABSTRACT: Purine radical cations ($dA^{\bullet+}$ and $dG^{\bullet+}$) are the primary hole carriers of DNA hole migration due to their favorable oxidation potential. Much less is known about the reactivity of higher energy pyrimidine radical cations. The thymidine radical cation ($T^{\bullet+}$) was produced at a defined position in DNA from a photochemical precursor for the first time. $T^{\bullet+}$ initiates hole transfer to dGGG triplets in DNA. Hole localization in a dGGG sequence accounts for ∼26% of $T^{\bullet+}$ formed under aerobic conditions in **9**. Reduction to yield thymidine is also quantified. 5-Formyl-2′-deoxyuridine is formed in low yield in DNA when $T^{\bullet+}$ is independently generated. This is inconsistent with mechanistic proposals concerning product formation from electron transfer in poly(dA−T) sequences, following hole injection by a photoexcited anthraquinone. Additional evidence that is inconsistent with the original mechanism was obtained using hole injection by a photoexcited anthraquinone in DNA. Instead of requiring the intermediacy of $T^{\bullet+}$, the strand damage patterns observed in those studies, in which thymidine is oxidized, are reproduced by independent generation of 2′-deoxyadenosin-*N*6-yl radical ($dA^{\bullet}$). Tandem lesion formation by $dA^{\bullet}$ provides the basis for an alternative mechanism for thymidine oxidation ascribed to hole migration in poly(dA−T) sequences. Overall, these experiments indicate that the final products formed following DNA hole transfer in poly(dA−T) sequences do not result from deprotonation or hydration of $T^{\bullet+}$, but rather from deprotonation of the more stable $dA^{\bullet+}$, to form $dA^{\bullet}$, which produces tandem lesions in which 5′-flanking thymidines are oxidized.

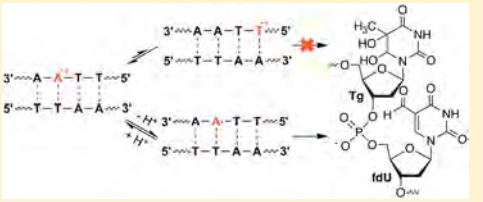

INTRODUCTION

DNA hole migration is initiated by one-electron oxidation of DNA, that is, hole injection, and is a primary consequence of the direct effect of ionizing radiation.[1−7] Hole injection by chemical and/or photochemical methods takes advantage of the differences in redox potentials to selectively generate the radical cation of 2′-deoxyguanosine (dG) and/or dA.[8−11] Short wavelength UV-irradiation (≤254 nm) and other forms of ionizing radiation (e.g., γ-radiolysis, photosensitization) are unselective and generate pyrimidine (e.g., $T^{\bullet+}$) and purine radical cations.[12−17] Nucleotide radical cation formation is a hallmark of the direct effect of ionizing radiation. The role of $dG^{\bullet+}$ in hole migration and subsequent hole trapping by reacting with H_2O/O_2 is well documented.[18,19] The reactivity of $T^{\bullet+}$ is less well understood than that of $dG^{\bullet+}$ and $dA^{\bullet+}$, due to the lack of methods to selectively produce the pyrimidine radical cation.[20] Most reports on $T^{\bullet+}$ reactivity have focused on the nucleoside. However, in a series of papers, $T^{\bullet+}$ was invoked as a direct precursor to products formed in electron transfer studies within poly(dA−T) sequences.[21−25] We wish to report on $T^{\bullet+}$ reactivity at a defined site in DNA for the first time via its independent generation from a photochemical precursor. In addition to providing insight into the competitive pathways for $T^{\bullet+}$ reactivity in DNA, these studies lead to an alternative mechanism for final products resulting from thymidine oxidation upon one-electron oxidation in poly(dA−T).

Monomeric $T^{\bullet+}$ undergoes four competing reactions (Scheme 1).[12,15−17] In DNA, these processes must compete with hole migration. Hydration (**1**) occurs preferentially at C6, and, when carried out in the presence of O_2 and reducing agent, ultimately yields thymidine glycol (Tg). Deprotonation from the C5-methyl group (**2**) under aerobic conditions ultimately yields 5-formyl-2′-deoxyuridine (fdU). Direct reduction to restore thymidine has a large driving force and occurs directly, as well as via N−H deprotonation (**3**), followed by formal hydrogen transfer. The relative rates for these competing processes vary, particularly with respect to the contributions of the deprotonation and hydration pathways. Furthermore, it is often difficult to quantify the contribution of the pathways that yield thymidine because most methods generate $T^{\bullet+}$ from the nucleoside via one-electron oxidation. However, recently, $T^{\bullet+}$ was produced from a photochemical precursor (**4**) other than thymidine.[20] Irradiation (350 nm) of **4** produces an intermediate radical (**5**) that undergoes β-heterolysis to produce $T^{\bullet+}$ (Scheme 2).[26−30] Generating monomeric $T^{\bullet+}$ from **4** revealed that thymidine is the major product under aerobic conditions, even in the absence of exogenous reducing agent. Products attributable to $T^{\bullet+}$ hydration are formed in ∼1/3 the yield of thymidine. Hydration (NMe-Tg) competed more effectively with reduction (NMe-T) when the respective radical cation was generated from NMe-**4**

Received: May 25, 2018

DOI: 10.1021/jacs.8b05484
J. Am. Chem. Soc. XXXX, XXX, XXX−XXX

Scheme 1. Thymidine Radical Cation Reactivity

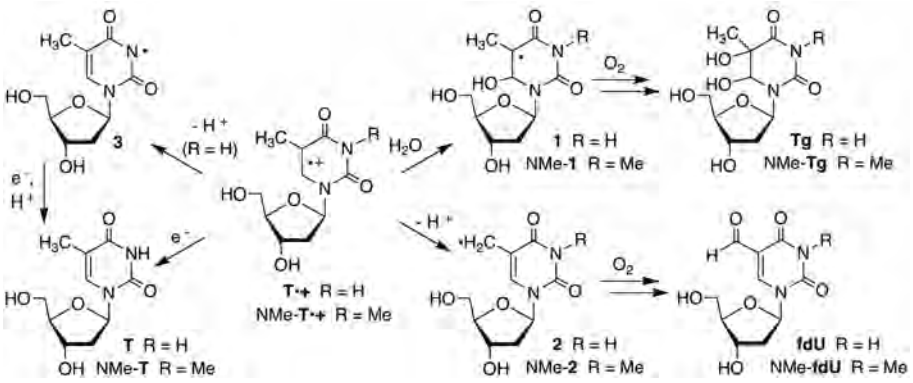

Scheme 2. Independent Generation of the Thymidine Radical Cation

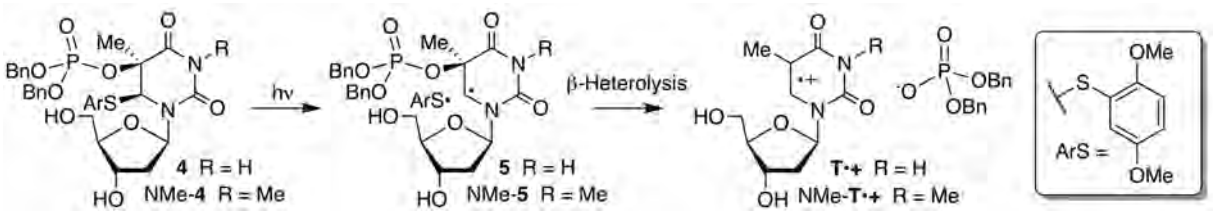

(via NMe-**5**), suggesting that N−H deprotonation contributed significantly to thymidine formation from $T^{\bullet+}$. However, the corresponding nucleosides attributable to C5-methyl deprotonation (fdU, NMe-fdU) were minor products from both precursors.

The low yield of (NMe-)fdU is contrary to some studies on monomeric $T^{\bullet+}$. It also is inconsistent with product studies upon electron transfer in poly(dA−T) sequences. Elegant studies by Schuster showed that when poly(dA−T) sequences are oxidized by a tethered photoexcited anthraquinone, the holes migrate through the duplex. The final sites of oxidation, detected via denaturing polyacrylamide gel electrophoresis (PAGE), following alkaline treatment, are at thymidine.[21−23] This is surprising because $dA^{\bullet+}$ is ∼3.5−6.5 kcal/mol more stable than $T^{\bullet+}$.[31,32] Preferential damage at thymidine was rationalized by a kinetic preference for deprotonation from the C5-methyl of $T^{\bullet+}$, ultimately resulting in the formation of fdU and 5-hydroxymethyl-2′-deoxyuridine (hmU). Tg detected in these experiments was attributed to $T^{\bullet+}$ hydration. The reactivity of independently generated $T^{\bullet+}$ within DNA described herein corroborates the observations reported concerning the monomeric radical cation. C5-Methyl deprotonation is a minor contributor to $T^{\bullet+}$ reactivity in DNA. An alternative mechanism involving formation of $dA^{\bullet}$ via deprotonation of the more stable $dA^{\bullet+}$ is put forth and tested using sequences similar to those employed in Schuster's original studies.[33] Finally, the alternative mechanism for product formation in one-electron oxidized poly(dA−T) is tested using the anthraquinone method for hole injection.

RESULTS AND DISCUSSION

Validation of 6 as a Photochemical Precursor for $T^{\bullet+}$ and Its Incorporation in Oligonucleotides. Photochemical generation of $T^{\bullet+}$ in aqueous solution proceeded cleanly.[20] However, the dibenzyl phosphate triester present in **4** proved to be unstable to the standard alkaline conditions (e.g., concentrated aqueous ammonia) used to deprotect chemically synthesized oligonucleotides. Consequently, we synthesized chemically stable diethyl phosphate triesters **6** and NMe-**6**. We also synthesized the corresponding 5′-benzoates (Bz-**6**, Bz-NMe-**6**). Bz-**6** and Bz-NMe-**6** were used to validate that the radical cation is produced (Tables S1 and S2). The benzoyl group provides a useful chromophore for UV-absorbance detection and quantification of products. Photolyses of Bz-**6** and Bz-NMe-**6** provided results similar to those of product studies from irradiation of **4** and NMe-**4**.[34] Mass balances from Bz-**6** photolyses ranged from 65% to 79%, depending upon solvent and pH. Thymidine was the major product formed from Bz-**6**, and the combined yields of hydration products increased significantly in photolyzates of Bz-NMe-**6** (28.3%), where N−H deprotonation is not possible, as compared to those of Bz-**6** (11.3%). In the absence of β-mercaptoethanol (BME, 10 mM), hydration products were formed in slightly higher yield than NMe-T from Bz-NMe-**6**, but the latter was favored by more than 3:1 when the photolysis was carried out in the presence of BME. Importantly, products resulting from C5-methyl deprotonation (e.g., 5′-benzoylated fdU or 5′-benzoylated NMe-fdU) were minor products (<4%) under all reaction conditions.

The diethyl phosphate triester in **6** was stable to solid-phase oligonucleotide synthesis and deprotection conditions, enabling the use of phosphoramidite **7** as a vehicle for introducing the radical cation precursor at defined sites in oligonucleotides. Oligonucleotides containing **6** were prepared using slight modifications of typical protocols. (Please note that for convenience the same numbering is used for molecules as monomeric nucleosides and in oligonucleotides.) Commercially available "fast deprotecting" phosphoramidites were used for introducing dA and dG. The phosphoramidite was coupled for 5 min, and acetic anhydride was replaced as a capping agent by pivalic anhydride.[35] The oligonucleotides were deprotected and cleaved from the solid-phase support using concentrated aqueous ammonia at room temperature for 12 h. Following purification by denaturing polyacrylamide gel electrophoresis, the oligonucleotides were characterized by mass spectrometry.[34]

DOI: 10.1021/jacs.8b05484
J. Am. Chem. Soc. XXXX, XXX, XXX−XXX

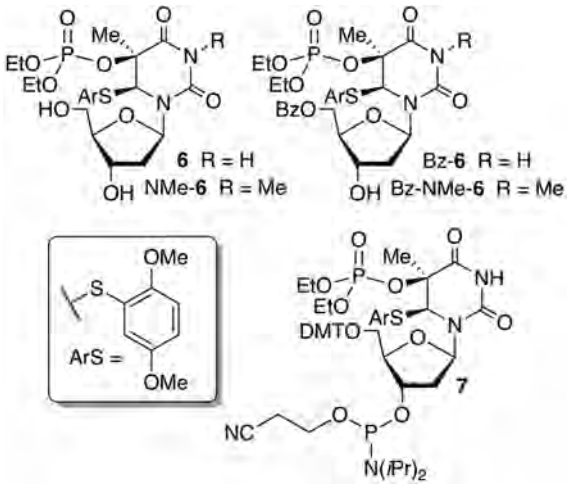

Thymidine Radical Cation ($T^{\bullet+}$) Reactivity in DNA. A series of duplexes (**8a,b**–**10a,b**) were prepared to examine $T^{\bullet+}$ generation and reactivity. Each of these duplexes contained at least one dGGG sequence, an often-used reporter group for hole transfer.[36−38] This trinucleotide sequence has the lowest ionization potential of any trinucleotide sequence and serves as a hole trap in DNA.[31] Hole trapping is typically detected as a strand break via denaturing PAGE following alkaline (piperidine) treatment or incubation with a base excision repair enzyme (e.g., formamidopyrimidine DNA glycosylase, Fpg). Furthermore, characteristic strand damage resulting from hole transfer is preferentially observed at the middle and 5′-dG of the trinucleotide sequence. The duplexes were designed to contain the dGGG sequence on the strand opposite that in which $T^{\bullet+}$ is produced. The efficiency for hole trapping has been estimated to be ∼8%.[36] Hence, the level of hole migration is actually ∼12-fold higher than the strand cleavage reported below. Time course studies were carried out to establish the irradiation time (75 min) needed to reach maximum conversion of **6** (Figure S3). Strand damage levels reported were corrected for background cleavage in unphotolyzed samples, as well as for damage in substrates containing thymidine (**8b**–**10b**) at the position where **6** is incorporated in otherwise identical duplexes.

5′-d(AGC TGC TTA T$G_{11}G_{12}$ G_{13}CA C$G_{17}G_{18}$ G_{19}TA TTG CTA GCT)
3′-d(TCG ACG AAT A C C C GX G C C C AT AAC GAT CGA) **8a,b**

5′-d(ACG TTC ATG TTA TTG_{15} AG_{17}T $G_{19}G_{20}$ G_{21} TTA TGT TGA)
3′-d(TGC AAG TAC AAT AA C X C A C C C AAT ACA ACT) **9a,b**

5′-d(CAT AAT ATT AAC G_{15}AT $G_{16}G_{17}G_{18}$ TAT TAT ATT AGC)
3′-d(GTA TTA TAA TXG C TA C C C ATA ATA TAA TCG) **10a,b**

a X = **6**; b X = T

Following UV-photolysis and piperidine treatment, strand damage (background subtracted)[34] was approximately equal within dG_{11-13} (0.63 ± 0.14%) and dG_{17-19} (0.70 ± 0.22%) within **8a** (Figure S4). In addition, the preference for strand damage within each triplet (dG_{12} > dG_{11} ≫ dG_{13}, dG_{18} ≈ dG_{17} ≫ dG_{19}) was consistent with the expectations of damage resulting from hole transfer (Figure 1A).[34] Overall, the damage detected at the two trinucleotide reporter sequences corresponds to ∼16% of the possible $T^{\bullet+}$ that can be produced.

Similarly, construct **9a** was designed to probe hole transfer from $T^{\bullet+}$ to dGs located at the complementary strand. Strand damage in **9a** was also consistent with the expectations for hole transfer (Figure 1B). Alkaline cleavage within dG_{19-21} was significantly greater than that at dG_{15} or dG_{17}, and although the

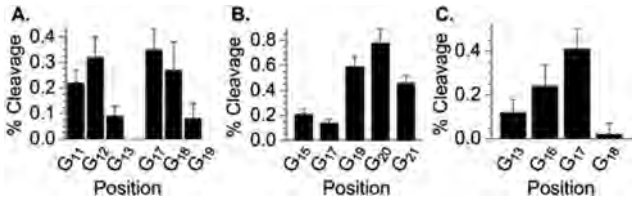

Figure 1. Strand damage due to hole migration from $T^{\bullet+}$. (A) **8a**, (B) **9a**, (C) **10a**. The data are the av ± std dev of three replicates.

preference for strand scission at dG_{20} and dG_{19} relative to dG_{21} was not as great as that in **8a**, the expected pattern resulting from hole transfer was observed (Figure S5). The total hole transfer detected over the 5 dGs was ∼26% of the possible radical cation produced.

Finally, substrate **10a** was designed to most closely match that employed by Giese where he established hole trapping efficiency. Substrate **10a** also enabled estimating the fraction of $T^{\bullet+}$ resulting in hole transfer by incorporating **6** within a sequence such that a restriction site for *Mse*I (5′-d(TTAA/AATT)) is created when thymidine is produced at that position.[36] *Mse*I does not cleave **10a** prior to photolysis (Figures S6 and S7). In addition, although we cannot rule out the possibility that hmdU and fdU were also substrates for *Mse*I, other experiments presented above and later in this report indicate that these products are formed in minor amounts. Thymidine is produced from reduction of $T^{\bullet+}$, which occurs upon hole transfer but can also be produced via other pathways. *Mse*I cleaves 36.4 ± 2.5% of photolyzed **10a**. The sum-total of piperidine-induced cleavage at dG_{13} and dG_{16-18} is 0.79 ± 0.26%, which when adjusted for 8% hole trapping efficiency accounts for 26.9% of the thymidine produced (Figure 1C).

5′-d(TTT TTT TTT ATA 6T_{14}A TAT ATT TTT TTT TTT)
3′-d(AAA AAA AAA TAT A A T ATA TAA AAA AAA AAA) **11**

5′-d(TTT TTT TTT ATA 6U_{14}A TAT ATT TTT TTT TTT)
3′-d(AAA AAA AAA TAT A A T ATA TAA AAA AAA AAA) **12**

In addition to alkali-labile strand scission at dG's due to hole transfer and thymidine formation, piperidine-induced cleavage was observed at the original $T^{\bullet+}$ generation site (44.3 ± 0.4%) in 5′-^{32}P-**10a**. Overall, we accounted for ∼81% of the photolyzed **6** in the substrate.

The reactivity of $T^{\bullet+}$ was also examined in duplexes lacking dG (**11**, **12**). Previous studies involving DNA hole transfer in poly(dA−T) sequences in which hole injection was induced via photoexcitation of anthraquinones led to the proposal that $T^{\bullet+}$ was the precursor to the observed alkali-labile lesions.[21−25] Product formation from the pyrimidine radical cation that is higher in energy than $dA^{\bullet+}$ was rationalized on the basis of kinetic over thermodynamic selectivity. In a dinucleotide step within poly(dA−T), alkali-labile lesion formation was highly dependent upon the flanking pyrimidine.[22] For instance, alkaline-labile cleavage was observed predominantly at the 5′-thymidine in a TT step, but no damage was detected at 5′-d(TU) sequences. 5′-d(UT) sequences provided yet a different pattern, as damage at the two nucleotides was approximately equal. LC−MS analysis of the nucleosides released upon enzyme digestion of the photolyzed oligonucleotides revealed fdU and Tg (see Scheme 1 for structures.). The authors proposed a mechanism to explain the sequence dependence, as well as the formation of fdU and Tg from $T^{\bullet+}$ (Scheme 3). The absence of any alkaline-labile lesions at 5′-d(TU) steps was surprising. If

DOI: 10.1021/jacs.8b05484
J. Am. Chem. Soc. XXXX, XXX, XXX−XXX

Scheme 3. Previously Proposed $T^{\bullet+}$ Reactivity

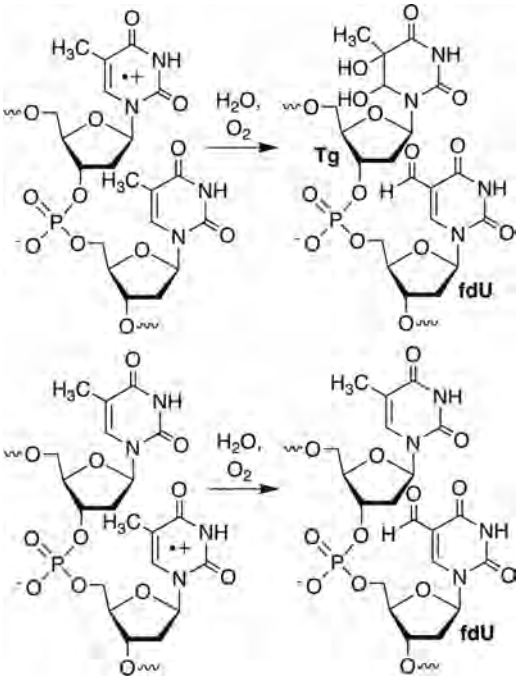

$T^{\bullet+}$ is generated, why would it undergo C5-methyl deprotonation to yield fdU, but not trapping by H_2O and O_2 to produce alkaline-labile Tg when flanked by a 3′-dU?

Denaturing PAGE analysis of 5′-^{32}P-**11** produced a piperidine-induced strand cleavage pattern that is qualitatively consistent with that previously reported (Figure S8). The major site of cleavage was at the nucleotide where $T^{\bullet+}$ was originally generated (49.3 ± 1.1%), and approximately 10.4 ± 0.1% strand damage was observed at T_{14}. If the 5′-Tg-fdU tandem lesion (Scheme 3) was formed as proposed, one would expect strand scission at the 5′-nucleotide to predominate because it is closer to the ^{32}P-label.[22] Furthermore, fdU is inefficiently cleaved by piperidine.[39] It is more difficult to reconcile the observation of comparable levels of strand damage at the radical cation site in 5′-^{32}P-**12** (46.6 ± 2.4%), and no damage was at dU_{14}. Formation of fdU as the major product (Scheme 3) is a foundation of the existing mechanism. Because fdU is inefficiently cleaved by piperidine, we utilized the glycosylase, hSMUG1, followed by NaOH to detect this modified nucleotide (Figure S8).[39,40] fdU was not detected in the photolyzate of **11**. This is also inconsistent with the previously proposed mechanism, but consistent with product studies on monomeric $T^{\bullet+}$, which showed that fdU is a minor product.[20,22]

We propose that the major site of alkaline lability is the position at which $T^{\bullet+}$ is independently generated. The major product(s) results from trapping by water regardless of the 3′-flanking nucleotide (Scheme 1). Moreover, the lack of influence of a flanking dU on alkali-labile strand scission when $T^{\bullet+}$ is flanked by a 3′-pyrimidine is very different from the results obtained using anthraquinone containing duplexes.[22] We believe that this difference is because $T^{\bullet+}$ is not produced upon photooxidation of DNA by anthraquinone.

An Alternative Mechanism for Alkaline-Labile Lesion Formation from Hole Transfer in Poly(dA−T) Sequences. The failure of independently generated $T^{\bullet+}$ to reproduce the products observed when holes were injected into poly(dA−T) duplexes via photoexcited anthraquinone led us to consider an alternative mechanism.[21−25] Because the preferential involvement of the pyrimidine radical cation versus the more stable $dA^{\bullet+}$ was initially a surprise, we considered whether the purine radical may provide an alternative explanation for the observed products. Recently, $dA^{\bullet}$ and $dA^{\bullet+}$ were shown to equilibrate in duplex DNA in a sequence-dependent manner (Scheme 4).[33,41]

Scheme 4. DNA Damage from dA Reactive Intermediates

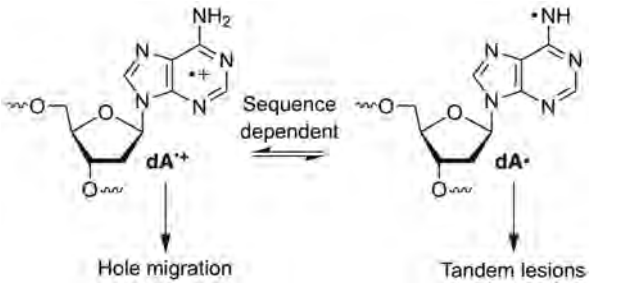

As expected, the latter gives rise to hole transfer, which localizes at dGGG sites. In the absence of such hole sinks, such as in poly(dA−T) substrates, one might expect that the migrating holes are carried by $dA^{\bullet+}$, which can deprotonate to form $dA^{\bullet}$. $dA^{\bullet}$ has been shown to selectively abstract the C5-methyl hydrogen from the 5′-adjacent thymidine, which led to the formation of tandem lesions in 5′-d(GT) sequences.[41]

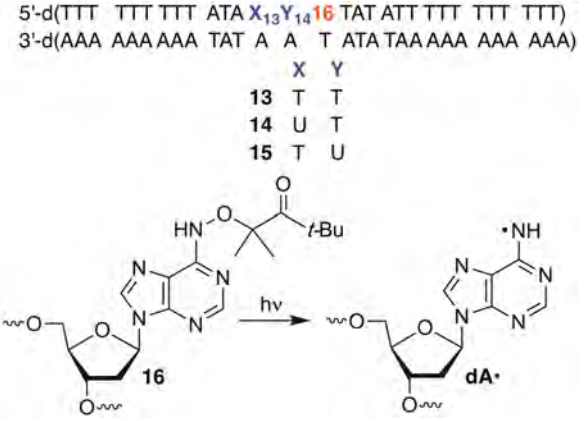

TT steps, such as those present in previously studied substrates, are well-positioned to react with 3′-$dA^{\bullet}$.[22] Consequently, we tested the possibility that $dA^{\bullet}$ is the species directly responsible for the products observed following hole injection in poly(dA−T) substrates. Substrates **13**−**15** were prepared containing one of the three aforementioned pyrimidine−pyrimidine steps flanked by a photochemical precursor (**16**) for $dA^{\bullet}$.[42] The $dA^{\bullet}$ precursor was not flanked by dA, so as to minimize $dA^{\bullet+}$ formation under the reaction conditions. Piperidine treatment of photolyzed 5′-^{32}P-**13**−**15** produced cleavage patterns that were fully consistent with those reported when duplexes containing the same dinucleotide steps and anthraquinone were irradiated (Figure 2). Specifically, duplex **13**, containing a 5′-T_{13}-T_{14}-$dA^{\bullet}$ sequence, results in predominant cleavage at the 5′-thymidine of the dinucleotide sequence. Similarly, strand damage is detected in approximately equal amounts at dU_{13} and T_{14} in 5′-^{32}P-**14**, whereas no damage is detected in the duplex (**15**) containing 5′-T-dU-$dA^{\bullet}$.

A mechanism that is consistent with these observations and previously characterized $dA^{\bullet}$ reactivity involves initial hydrogen atom abstraction from the C5-methyl group of the thymidine

DOI: 10.1021/jacs.8b05484
J. Am. Chem. Soc. XXXX, XXX, XXX−XXX

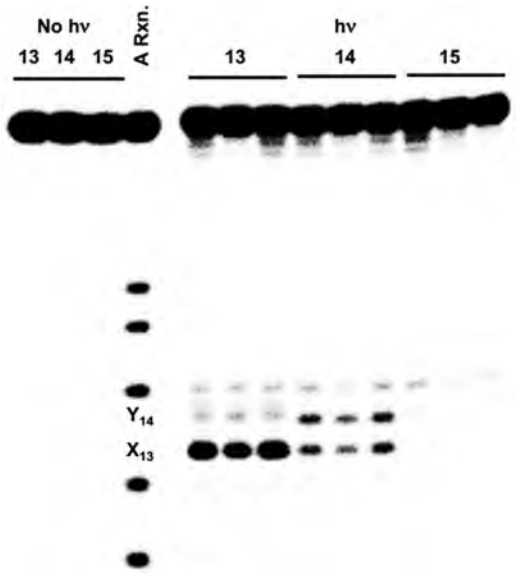

Figure 2. Strand damage in duplexes (5′-^{32}P-**13**−**15**) containing 5′-pyr-pyr-dA•. Three replicates are shown for each substrate.

bonded to the 5′-phosphate of the neutral nitrogen radical (Scheme 5). Under the aerobic conditions, the 5-(2′-deoxyuridinyl)-methyl peroxyl radical (Tp•) reacts with the 5′-adjacent pyrimidine by adding to the pyrimidine double bond at position 13. Addition at the C6-position of thymidine is shown. However, we cannot distinguish between this pathway and addition to the C5-position. Tp• addition to the 5′-adjacent pyrimidine may also explain why alkali-labile strand damage at the 5′-nucleotide in a 5′-d(UT) sequence is less favored than in a 5′-d(TT) sequence. The presence of a C5-proton in the former can give rise to products such as 5-hydroxy-2′-deoxyuridine, which do not yield strand scission upon alkali treatment.[43−45] Furthermore, previous investigations in which pyrimidine peroxyl radicals are independently generated in duplex DNA have shown that alkali-labile lesion formation at a 5′-dU is less efficient than when thymidine is present at this position.[46] We also cannot rule out contributions from pathways in which Tp• is ultimately converted to fdU, which is observed when photo-excited anthraquinone is the source of damage but not when T•+ is independently generated in DNA.[22] Importantly, hydrogen atom abstraction from the thymidine C5-methyl group by dA• explains why strand damage at 5′-d(TU) sequences is not detected in experiments utilizing anthraquinone modified DNA.

This mechanism was further validated via LC−MS/MS analysis of photolyzates of **17**. A dodecameric substrate was employed to ensure detection of fragments via collision-induced dissociation (CID), which is crucial for product assignment.[47−49] The complementary strand contained two additional thymidines to facilitate separation on the LC. Substrate **17**

Scheme 5. Tandem Lesion Formation from dA•

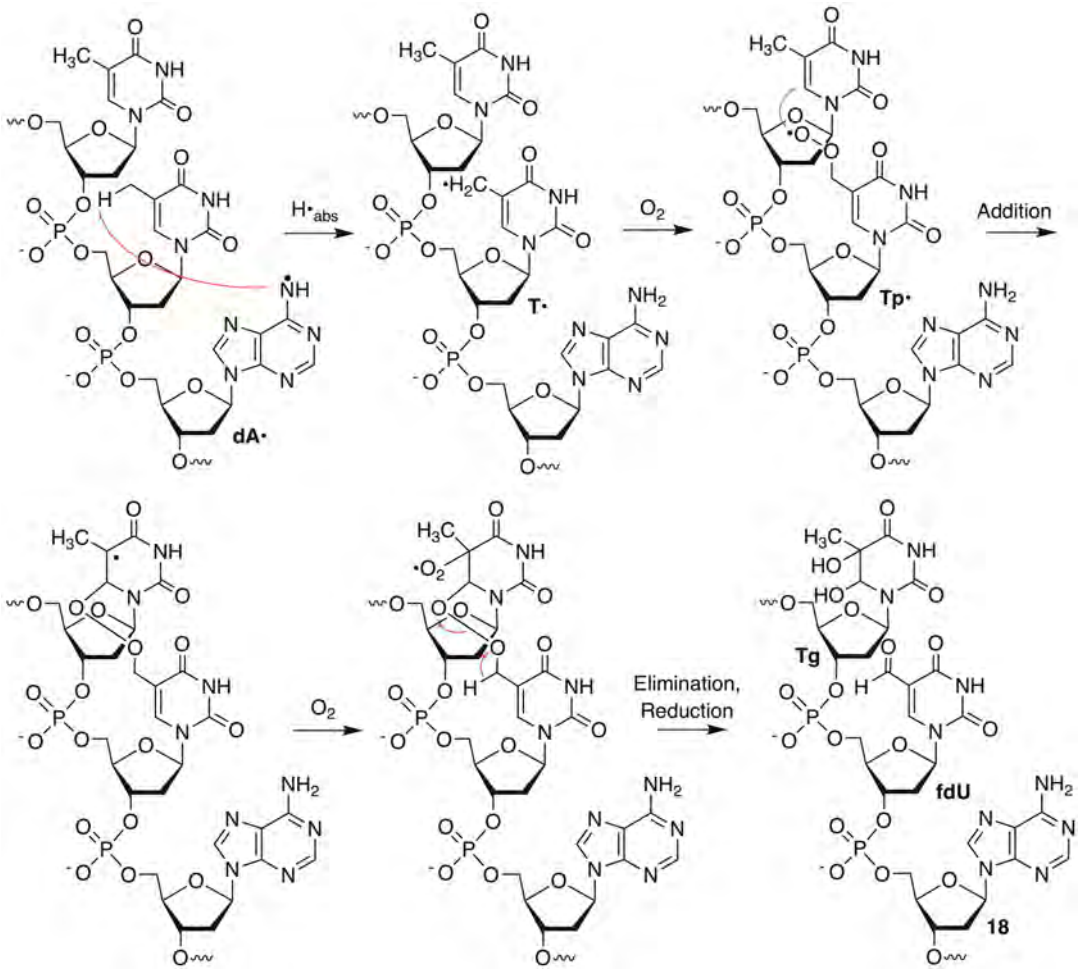

DOI: 10.1021/jacs.8b05484
J. Am. Chem. Soc. XXXX, XXX, XXX−XXX

contained dG−dC base pairs to stabilize the duplex (T_m = 35.5 °C) against melting during photolysis. If the products are due to the intermediacy of dA$^{\bullet}$, the presence of dG−dC base pairs should not influence the chemistry. The observation of an identical damage pattern in **20** and **13**, despite the presence of multiple dG−dC base pairs, is consistent with this hypothesis (Figure S10).

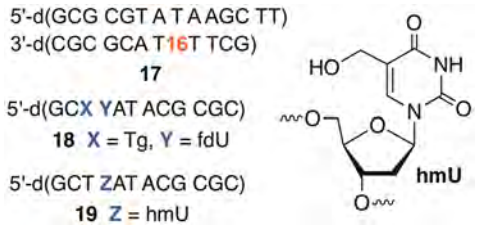

A product (**18**) with m/z = 3666.6240 that is consistent with the expected mass and fragmentation pattern for the tandem lesion containing 5′-d(Tg-fdU) and dA at the position where dA$^{\bullet}$ was generated was observed (Figure 3). Furthermore, the fragment [a_3 − 143 Da], which is characteristic for Tg-containing DNA, is detected by LC−MS/MS (Figure S14).[50] Finally, photolysis of **17** in the presence of β-mercaptoethanol (1 mM) eliminates formation of **18**, and only **19** is observed. This is consistent with the intermediacy of Tp$^{\bullet}$ in tandem lesion formation.

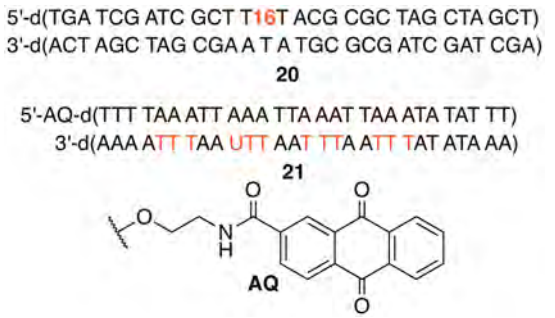

The above observations suggested an experiment to distinguish between the mechanism involving T$^{\bullet+}$ and that proposed herein involving dA$^{\bullet}$. We utilized the anthraquinone system to photochemically induce oxidative damage. It was previously shown that when photoexcited anthraquinone was used to introduce holes, 5′-d(TTT) sequences were preferentially damaged at the central thymidine, followed by the 3′-terminal T.[21,22] One of the four 5′-d(TTT) steps in a previously reported substrate was substituted by a 5′-d(TTU) sequence. If the mechanism involves T$^{\bullet+}$, the TT step in 5′-d(TTU) should give rise to a tandem lesion because the hole transferred from the dA$^{\bullet+}$ on the opposite strand will not be affected by the presence of dU. If the alternative mechanism proposed above is responsible for the products, substituting a single dU for thymidine at the 3′-terminus of a 5′-d(TTT) sequence should eliminate strand damage at that location because the 3′-adjacent dA$^{\bullet}$ radical responsible for initiating tandem lesion formation will not have a C5-methyl hydrogen atom to abstract. Indeed, photolysis of 5′-^{32}P-**21** generated the previously reported strand damage pattern in 5′-d(TTT) upon piperidine treatment (Figure 4). Moreover, no damage was detected at the 5′-d(TTU) sequence. Furthermore, piperidine treatment of photolyzed 5′-^{32}P-**22** and 5′-^{32}P-**23** reproduced the reactivity disparity between 5′-d(TTT) and 5′-d(TTU) (Figure S11).

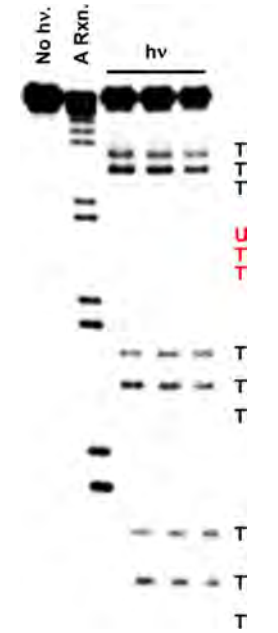

Figure 4. Alkali-labile strand damage in 5′-^{32}P-**21** following photolysis for 8 h.

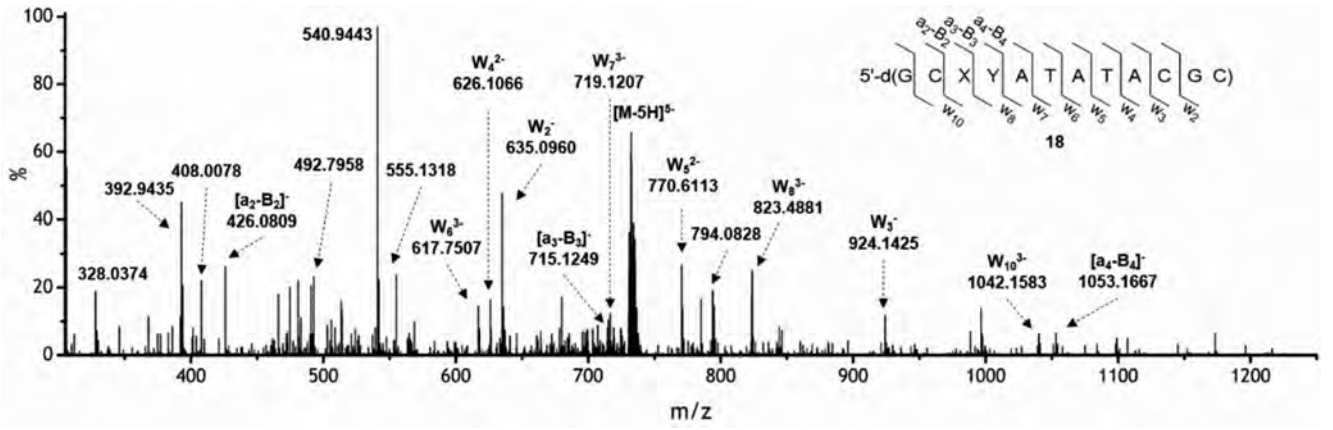

Figure 3. CID mass spectrum of the ion (m/z = 732.7, z = 5) of tandem lesion **18**. X = Tg, Y = fdU.

DOI: 10.1021/jacs.8b05484
J. Am. Chem. Soc. XXXX, XXX, XXX−XXX

The alternative mechanism proposed (Scheme 5) is consistent with all of these observations.

5'-d(TTT TTT TTA TAT TX16 TAT ATT TTT TTT TTT)
3'-d(AAA AAA AAT ATA A A T ATA TAA AAA AAA AAA)
22 X = U
23 X = T

CONCLUSIONS

Radical cations ("holes") are important intermediates in DNA damage imparted by the direct effect of ionizing radiation. Chemists have employed clever ways to produce holes in DNA, but these usually involve generating lower energy purine radical cations, as opposed to pyrimidine radical cations. Using a photochemical precursor, a pyrimidine radical cation ($T^{\bullet+}$) was independently generated at a defined site within DNA for the first time. $T^{\bullet+}$ engages in hole transfer, but is also trapped by water to produce alkaline-labile lesions. $T^{\bullet+}$ does not yield detectable levels of fdU in DNA. This is consistent with studies on monomeric $T^{\bullet+}$ in which fdU was a minor product.[42]

$T^{\bullet+}$ reactivity in DNA composed of only dA and T was inconsistent with previous proposals concerning the involvement of this species when the photoexcited state of anthraquinone was used to introduce a hole.[21−25] Combining observations made from independently generated $T^{\bullet+}$ with a photochemical method for producing $dA^{\bullet}$ at defined sites in DNA led to an alternative proposal for explaining the products of hole transfer in poly(dA−T) DNA.

Rather than utilizing the higher energy $T^{\bullet+}$, we propose that $dA^{\bullet+}$ holes migrate throughout the poly(dA−T) sequence (Scheme 6). Holes are fixed at a particular location upon

Scheme 6. $dA^{\bullet+}$ Holes Migrating Throughout the Poly(dA−T) Sequence

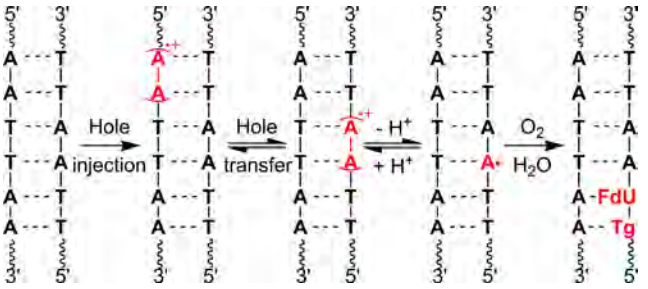

deprotonation of $dA^{\bullet+}$. The neutral-nitrogen radical ($dA^{\bullet}$) generates the observed products via tandem lesion formation. The tandem lesions are formed under aerobic conditions via initial hydrogen atom abstraction from the C5-methyl group of a 5′-adjacent thymidine, a process previously observed for $dA^{\bullet}$ (Scheme 5).[41] Independent generation of $dA^{\bullet}$ reproduced the sequence specificity of tandem lesion formation when holes are injected by photoexcited anthraquinones.[22] Finally, unlike the previously proposed mechanism, the alternative mechanism also predicted the lack of strand damage in a 5′-d(TTU) sequence using anthraquinone.

2′-Deoxyadenosin-*N*6-yl radical ($dA^{\bullet}$) was recently shown to be a traceless participant in tandem lesion formation in γ-radiolysis mediated DNA damage. The above experiments demonstrate that it plays a comparable role in DNA damage resulting from hole transfer within poly(dA−T) sequences.[33,41]

EXPERIMENTAL SECTION

Materials and Methods. THF was distilled over Na/benzophenone. DCM, TEA, DIPEA, DMF, and pyridine were dried over CaH_2. All other reagents were purchased from commercial sources and were directly used without further purification unless noted otherwise. T4 polynucleotide kinase (T4 PNK), human single-strand-selective monofunctional uracil-DNA glycosylase (hSMUG1), and restriction enzyme *Mse*I were obtained from New England Biolabs. γ-^{32}P-ATP was purchased from PerkinElmer. C18-Sep-Pak cartridges were obtained from Waters. Diethyl *N*,*N*-diethyl phosphoramidite was synthesized as described in the literature.[51] All reactions were carried out under argon atmosphere and monitored by TLC on silica gel G-25 UV254 (0.25 mm). Flash column chromatography was performed with Silicycle grade 70−230 mesh, 60−200 μm, 60 Å silica. The ratio between silica gel and crude product ranged from 100:1 to 20:1 (w/w). Samples in a mixture of acetonitrile and water/buffer (phosphate buffer (20 mM) or Chelex-treated pH = 5 citrate buffer (40 mM)) at a ratio of 1:1 (v/v) typically contain 100 μM precursor as well as 20 μM of the internal standard 5′-benzoyl-2′-deoxyuridine (BzdU). Photolyses were performed in Pyrex tubes in a Rayonet photoreactor fitted with 16 lamps with maximum output at 350 nm. Samples containing Bz-**6** were photolyzed for 30 min, while samples containing Bz-NMe-**6** were photolyzed for 45 min. Photolyzed samples of Bz-**6** were incubated at 37 °C in the presence of $MeONH_2$·HCl (10 mM) and NaOAc (10 mM) for 1 h. The samples were neutralized using pH 8.0 PBS buffer (100 mM, 12% volume of samples) prior to UPLC analysis. Photolyzed samples were analyzed using UPLC with an Acquity 1.8 μm C18 UPLC HSS column (100 × 2.1 mm). Detection was carried out at 230 nm, following separation using water (solvent A) and acetonitrile (solvent B) with the following linear gradient (0.2 mL/min): (time (min), %B) 0, 5; 30, 40; 35, 70; 40, 97; 42, 5; 45, 5. Response factors (R_f) for each compound (X) versus 5′-benzoyl-2′-deoxyuridine (BzdU) were calculated using the following formula: $([X]/[BzdU]) = R_f(A(X)/A(BzdU))$, where [X] is the concentration of compound X and [BzdU] is the concentration of BzdU. $A(X)$ and $A(BzdU)$ are the areas under the peaks corresponding to X versus BzdU. ESI−MS was carried out on a Thermoquest LCQDeca. UPLC−MS analyses were carried out on a Waters Acquity/Xevo-G2 UPLC-MS system equipped with an oligonucleotide BEH C18 column (130 Å, 1.7 μm, 2.1 mm × 100 mm). Oligonucleotide masses were obtained via deconvolution using MassLynx 4.1 software. CID was processed using Microsoft Excel. MALDI-TOF analyses were carried out on a Bruker AutoFlex III MALDI-TOF. Quantification of radiolabeled oligonucleotides was carried out using a Molecular Dynamics Phosphorimager 860 equipped with ImageQuant Version TL software.

Oligonucleotide Synthesis. Oligonucleotides were prepared on an Applied Biosystems Inc. 394 oligonucleotide synthesizer. Cyanoethyl phosphoramidites with phenoxyacetyl protecting groups on the exocyclic amines of dA and dG were used for the synthesis of unnatural oligonucleotides. For the synthesis of oligonucleotides containing **6**, the capping A reagent is the mixture of lutidine:trimethyl acetic anhydride:THF = 1:1:8.[35] The coupling time for modified phosphoramidite was increased to 5 min. All functionalized oligonucleotides were deprotected and cleaved from solid support with 28% aq NH_3 at room temperature. The deprotection times for oligonucleotides containing **6** and **16** are 12 and 16 h, repectively. The oligonucleotide containing anthraquinone **21** was synthesized according to the reported procedure.[52] The oligonucleotides are purified via 20% denaturing polyacrylamide gel electrophoresis (PAGE).

Photolysis of Oligonucleotides. The strand (1−2 μM) was labeled at the 5′ end with γ-^{32}P-ATP using T4 PNK in T4 PNK buffer (70 mM Tris-HCl, pH 7.6, 10 mM $MgCl_2$, 5 mM DTT, at least 90 min, 37 °C). The labeled strand was hybridized to the complementary strand (1.5 equiv) in PBS by heating at 90 °C for 1 min and slowly cooling to room temperature. The hybridized duplexes were diluted to 0.1 μM in PBS before photolysis. All photolyses were carried out in Pyrex tubes using a Rayonet photoreactor equipped with 16 lamps having a maximum output at 350 nm. Oligonucleotides containing **6** and **16** are photolyzed for 75 min and 8 h, respectively.

DOI: 10.1021/jacs.8b05484
J. Am. Chem. Soc. XXXX, XXX, XXX−XXX

Postphotolysis Treatments. Aliquots from photolyzed solutions or unphotolyzed controls were treated with piperidine (1 M, 30 min, 90 °C), *Mse*I (5 Units, 50 mM potassium acetate, 20 mM Tris-acetate, 10 mM magnesium acetate, 100 μg/mL BSA (pH 7.9), 1 h, 37 °C), hSMUG1 (5 Units, 50 mM potassium acetate, 20 mM Tris-acetate, 10 mM magnesium acetate, 100 μg/mL BSA (pH 7.9), 1 h, 37 °C), or NaOH (0.1 M, 30 min, 37 °C). NaOH treated samples were neutralized with HCl (1 equiv). All samples treated with enzymes were precipitated (0.3 M NaOAc, pH 5.2, 0.1 mg/mL calf thymus DNA) with ethanol. Piperidine treated samples were evaporated to dryness under vacuum, and washed with 2 × 10 μL water, which was also removed under vacuum. Samples were analyzed by dissolving in formamide loading buffer prior to analyzing by 20% denaturing PAGE. Piperidine solution was prepared freshly.

UPLC–MS/MS Analysis of Oligonucleotides. Photolyzates (8 μL) containing 5 μM of duplex dodecamer were analyzed by UPLC–MS using the oligonucleotide BEH C18 column (A, 100 mM HFIP and 8.6 mM TEA; B, methanol; 5% B from t = 0 to t = 5 min; 5–13% B linearly over 15 min; 13% B from t = 20 to t = 15 min; 9–30% B linearly over 5 min; 30% B from t = 25 to t = 30 min; 30–5% B linearly over 5 min; 5% B from t = 35 to t = 40 min; flow rate, 0.2 mL/min.). The column temperature was 60 °C. The collision energy was set to ramp from 10 to 45 V.

(5*R*,6*S*)-Bis-TBDMS-5,6-dihydro-5-diethyl Phosphate-6-(2,5-dimethoxythiophenyl)-thymidine (TBS-6). Diethyl *N*,*N*-diethyl phosphoramidite (46.4 mg, 0.24 mmol) was added to a solution of (5*R*,6*S*)-bis-TBDMS-5,6-dihydro-5-hydroxy-6-(2,5-dimethoxythiophenyl)-thymidine (131 mg, 0.20 mmol) in CH_2Cl_2 (2 mL) under argon, followed by ethyl-thio-tetrazole (0.25 M in acetonitrile, 0.96 mL, 0.24 mmol). The solution was stirred at room temperature overnight and then cooled to 0 °C. *t*-BuOOH (5–6 M in decane, 0.3 mL) was added, and the mixture was stirred at 0 °C for 1 h. After being warmed to room temperature, the mixture was directly subjected to flash column chromatography on silica gel (EtOAc:CH_2Cl_2 = 1:3) to provide the product (82 mg, 51.8%) as a white foam. ^{1}H NMR (400 MHz, $CDCl_3$) δ 7.22 (s, 1H), 7.08 (d, J = 3.1 Hz, 1H), 6.88 (dd, J = 9.0, 3.1 Hz, 1H), 6.77 (d, J = 9.0 Hz, 1H), 6.15 (dd, J = 9.4, 5.3 Hz, 1H), 5.30 (s, 1H), 4.24–4.12 (m, 5H), 3.77 (s, 3H), 3.75 (s, 3H), 3.70–3.66 (m, 1H), 3.54–3.49 (m, 1H), 3.14–3.01 (m, 1H), 2.45–2.38 (m, 1H), 1.85 (s, 3H), 1.68–1.63 (m, 1H), 1.32–1.29 (m, 6H), 0.90 (s, 9H), 0.88 (s, 9H), 0.08 (s, 6H), 0.06 (s, 3H), 0.05 (s, 3H). ^{13}C NMR (101 MHz, $CDCl_3$) δ 167.6, 167.5, 155.1, 153.2, 150.2, 123.3, 117.7, 117.1, 111.7, 86.3, 84.6, 79.2, 79.1, 72.7, 64.5, 64.2, 63.8, 63.5, 56.0, 55.8, 36.1, 30.0, 26.0, 25.8, 22.7, 18.4, 18.0, 16.1, 16.0, −4.7, −4.8, −5.4. ^{31}P NMR (162 MHz, $CDCl_3$) δ −5.89. HRMS (ESI-TOF) m/z: $[M + H]^+$ calcd for $C_{34}H_{62}N_2O_{11}PSSi_2$ 793.3350; found 793.3344.

(5*R*,6*S*)-5,6-Dihydro-5-diethyl Phosphate-6-(2,5-dimethoxythiophenyl)-thymidine (6). $Et_3N{\cdot}3HF$ (290 mg, 1.8 mmol) was added to a solution of (5*R*,6*S*)-3′,5′-bis-TBDMS-3-methyl-5,6-dihydro-5-diethyl phosphate-6-(2,5-dimethoxythiophenyl)-thymidine (79.2 mg, 0.1 mmol) in THF (3.0 mL). The mixture was stirred at room temperature overnight, at which time the solvent was removed under reduced pressure. The residue was purified by flash column chromatography on silica gel (methanol:CH_2Cl_2 = 1:9) to afford the product **6** (47 mg, 83%) as a white foam. ^{1}H NMR (400 MHz, $CDCl_3$) δ 7.46 (s, 1H), 7.06 (d, J = 3.1 Hz, 1H), 6.90 (dd, J = 9.0, 3.1 Hz, 1H), 6.77 (d, J = 9.0 Hz, 1H), 6.17 (dd, J = 9.0, 5.8 Hz, 1H), 5.96 (s, 1H), 4.37 (ddd, J = 11.1, 10.2, 8.8 Hz, 3H), 4.27–4.11 (m, 3H), 3.83 (d, J = 12.5 Hz, 2H), 3.76 (s, 3H), 3.74 (s, 3H), 3.68 (d, J = 11.3 Hz, 1H), 2.40 (dd, J = 8.6, 5.3 Hz, 2H), 1.85 (s, 3H), 1.66–1.61 (m, 1H), 1.39–1.34 (m, 6H). ^{13}C NMR (101 MHz, $CDCl_3$) δ 167.8, 167.7, 155.7, 153.0, 150.6, 124.0, 117.8, 116.9, 111.7, 86.9, 85.6, 78.9, 72.8, 65.2, 64.8, 62.7, 62.3, 55.9, 36.9, 22.9, 16.1, 16.0. ^{31}P NMR (162 MHz, $CDCl_3$) δ −6.20. HRMS (ESI-TOF) m/z: $[M + H]^+$ calcd for $C_{22}H_{34}N_2O_{11}PS$ 565.1621; found 565.1631.

(5*R*,6*S*)-5′-DMT-5,6-dihydro-5-diethyl Phosphate-6-(2,5-dimethoxythiophenyl)-thymidine (DMT-6). Nucleoside **6** (141.1 mg, 0.25 mmol) was azeotropically coevaporated with anhydrous pyridine (3 × 2 mL) and then redissolved in anhydrous pyridine (2 mL). 4,4′-Dimethoxytrityl chloride (127.1 mg, 0.375 mmol) and DMAP (6.11 mg, 0.05 mmol) were added at 0 °C under argon. The solution was allowed to warm to room temperature overnight. The reaction was quenched with MeOH (0.5 mL). The solvent was removed under reduced pressure and then diluted with ethyl acetate (40 mL). The mixture was washed with water (30 mL), brine (30 mL), dried over anhydrous Na_2SO_4, filtered, and concentrated. The residue was purified by flash column chromatography on silica gel (EtOAc:hexane = 1:1) to yield the product as a white foam (100 mg, 47.7%). ^{1}H NMR (400 MHz, $CDCl_3$) δ 7.68 (s, 1H), 7.47–7.37 (m, 2H), 7.37–7.24 (m, 6H), 7.23–7.15 (m, 1H), 7.06 (d, J = 3.1 Hz, 1H), 6.93–6.78 (m, 5H), 6.72 (d, J = 9.1 Hz, 1H), 6.12 (dd, J = 7.8, 6.5 Hz, 1H), 5.25 (s, 1H), 4.26 (d, J = 3.2 Hz, 1H), 4.22–3.96 (m, 4H), 3.82–3.72 (m, 7H), 3.71 (s, 3H), 3.66 (s, 3H), 3.40 (dd, J = 9.8, 5.2 Hz, 1H), 3.24 (dd, J = 9.8, 6.3 Hz, 1H), 2.71 (m, 1H), 2.37 (d, J = 2.5 Hz, 1H), 1.89 (m, 1H), 1.79 (s, 3H), 1.28 (m, 3H), 1.20 (m, 3H). ^{13}C NMR (101 MHz, $CDCl_3$) δ 171.2, 167.7, 167.6, 158.5, 155.1, 153.1, 150.3, 144.7, 135.9, 130.1, 128.1, 127.9, 126.9, 123.2, 117.7, 117.2, 113.2, 111.7, 86.5, 84.0, 83.4, 79.4, 79.3, 72.7, 64.5, 64.2, 64.1, 63.6, 60.4, 55.9, 55.8, 55.2, 35.8, 22.7, 21.1, 16.1, 14.2. ^{31}P NMR (162 MHz, $CDCl_3$) δ −6.05. HRMS (ESI-TOF) m/z: $[M + Na]^+$ calcd for $C_{43}H_{51}N_2NaO_{13}PS$ 889.2747; found 889.2740.

Phosphoramidite (7). Diisopropylethylamine (93.1 mg, 0.72 mmol) and cyanoethyl diisopropylphosphoramidic chloride (51.1 mg, 0.216 mmol) were added to a solution of DMT-**6** (150.9 mg, 0.18 mmol) in CH_2Cl_2 (3 mL) at 0 °C under argon. The mixture was stirred at 0 °C for 2 h. The solution was diluted with ethyl acetate (40 mL), and then washed with saturated $NaHCO_3$ (40 mL) and brine (30 mL). The organic phase was dried over anhydrous Na_2SO_4, and the solvent was removed under reduced pressure. The residue was purified by flash column chromatography on silica gel (CH_2Cl_2:ethyl acetate = 1:1, containing 1% Et_3N) to yield 7 (170 mg, 88.6%) as a white foam. ^{1}H NMR (400 MHz, $CDCl_3$) δ 7.44 (dd, J = 7.2, 4.4 Hz, 2H), 7.37–7.27 (m, 6H), 7.20 (dd, J = 7.3, 5.6 Hz, 2H), 7.07 (d, J = 3.1 Hz, 1H), 6.83 (ddd, J = 9.0, 5.9, 1.2 Hz, 5H), 6.78–6.69 (m, 1H), 6.24–6.06 (m, 1H), 5.28 (d, J = 7.1 Hz, 1H), 4.35 (dd, J = 6.6, 3.2 Hz, 1H), 4.13 (dd, J = 15.7, 13.7 Hz, 2H), 4.01 (d, J = 7.1 Hz, 3H), 3.78 (d, J = 3.4 Hz, 6H), 3.72 (d, J = 3.0 Hz, 3H), 3.66 (d, J = 7.4 Hz, 3H), 3.60 (d, J = 2.0 Hz, 3H), 3.39–3.17 (m, 2H), 2.65 (ddd, J = 21.6, 14.4, 6.6 Hz, 2H), 2.42 (t, J = 6.7 Hz, 1H), 2.04–1.88 (m, 1H), 1.85 (d, J = 2.5 Hz, 3H), 1.28 (ddd, J = 11.7, 8.9, 4.0 Hz, 4H), 1.20–1.10 (m, 12H), 1.06 (d, J = 6.8 Hz, 3H). ^{31}P NMR (162 MHz, $CDCl_3$) δ 148.73, 148.30, −5.93, −5.99. HRMS (ESI-TOF) m/z: $[M + Na]^+$ calcd for $C_{52}H_{69}N_4O_{14}P_2S$ 1067.4006; found 1067.3971.

■ ASSOCIATED CONTENT

Supporting Information

The Supporting Information is available free of charge on the ACS Publications website at DOI: 10.1021/jacs.8b05484.

Experimental procedures for the synthesis of NMe-compounds and Bz-**6**; and representative autoradiograms, expanded LC–MS/MS data analysis, and MS characterization of oligonucleotides containing modified nucleotides (PDF)

■ AUTHOR INFORMATION

Corresponding Author

*mgreenberg@jhu.edu

ORCID

Marc M. Greenberg: 0000-0002-5786-6118

Author Contributions

†H.S. and L.Z. contributed equally.

Notes

The authors declare no competing financial interest.

DOI: 10.1021/jacs.8b05484
J. Am. Chem. Soc. XXXX, XXX, XXX–XXX

■ ACKNOWLEDGMENTS

We are grateful for support from the National Institute of General Medicine (GM-054996). We thank Professor Jacqueline Barton and Dr. Phil Bartels for providing helpful suggestions concerning the manuscript.

■ REFERENCES

(1) von Sonntag, C. *Free-Radical-Induced DNA Damage and Its Repair*; Springer-Verlag: Berlin, 2006.
(2) Purkayastha, S.; Milligan, J. R.; Bernhard, W. A. *J. Phys. Chem. B* **2005**, *109*, 16967−16973.
(3) Yokoya, A.; Cunniffe, S. M. T.; O'Neill, P. *J. Am. Chem. Soc.* **2002**, *124*, 8859−8866.
(4) Banyasz, A.; Martínez-Fernández, L.; Balty, C.; Perron, M.; Douki, T.; Improta, R.; Markovitsi, D. *J. Am. Chem. Soc.* **2017**, *139*, 10561−10568.
(5) Ming, X.; Matter, B.; Song, M.; Veliath, E.; Shanley, R.; Jones, R.; Tretyakova, N. *J. Am. Chem. Soc.* **2014**, *136*, 4223−4235.
(6) Kanvah, S.; Joseph, J.; Schuster, G. B.; Barnett, R. N.; Cleveland, C. L.; Landman, U. *Acc. Chem. Res.* **2010**, *43*, 280−287.
(7) Ding, H.; Greenberg, M. M. *J. Am. Chem. Soc.* **2007**, *129*, 772−773.
(8) Genereux, J. C.; Barton, J. K. *Chem. Rev.* **2010**, *110*, 1642−1662.
(9) Genereux, J. C.; Wuerth, S. M.; Barton, J. K. *J. Am. Chem. Soc.* **2011**, *133*, 3863−3868.
(10) Harris, M. A.; Mishra, A. K.; Young, R. M.; Brown, K. E.; Wasielewski, M. R.; Lewis, F. D. *J. Am. Chem. Soc.* **2016**, *138*, 5491−5494.
(11) Fujitsuka, M.; Majima, T. *Chem. Sci.* **2017**, *8*, 1752−1762.
(12) Deeble, D. J.; Schuchmann, M. N.; Steenken, S.; von Sonntag, C. *J. Phys. Chem.* **1990**, *94*, 8186−8192.
(13) Geimer, J.; Beckert, D. *J. Phys. Chem. A* **1999**, *103*, 3991−3998.
(14) Wagner, J. R.; van Lier, J. E.; Johnston, L. J. *Photochem. Photobiol.* **1990**, *52*, 333−343.
(15) Malone, M. E.; Symons, M. C. R.; Parker, A. W. *J. Chem. Soc., Perkin Trans. 2* **1993**, 2067−2075.
(16) Shaw, A. A.; Voituriez, L.; Cadet, J.; Gregoli, S.; Symons, M. C. R. *J. Chem. Soc., Perkin Trans. 2* **1988**, 1303−1307.
(17) Adhikary, A.; Kumar, A.; Heizer, A. N.; Palmer, B. J.; Pottiboyina, V.; Liang, Y.; Wnuk, S. F.; Sevilla, M. D. *J. Am. Chem. Soc.* **2013**, *135*, 3121−3135.
(18) Rokhlenko, Y.; Cadet, J.; Geacintov, N. E.; Shafirovich, V. *J. Am. Chem. Soc.* **2014**, *136*, 5956−5962.
(19) Rokhlenko, Y.; Geacintov, N. E.; Shafirovich, V. *J. Am. Chem. Soc.* **2012**, *134*, 4955−4962.
(20) Sun, H.; Taverna Porro, M. L.; Greenberg, M. M. *J. Org. Chem.* **2017**, *82*, 11072−11083.
(21) Joy, A.; Ghosh, A. K.; Schuster, G. B. *J. Am. Chem. Soc.* **2006**, *128*, 5346−5347.
(22) Ghosh, A.; Joy, A.; Schuster, G. B.; Douki, T.; Cadet, J. *Org. Biomol. Chem.* **2008**, *6*, 916−928.
(23) Joseph, J.; Schuster, G. B. *Chem. Commun.* **2010**, *46*, 7872−7878.
(24) Barnett, R. N.; Joseph, J.; Landman, U.; Schuster, G. B. *J. Am. Chem. Soc.* **2013**, *135*, 3904−3914.
(25) Kanvah, S.; Schuster, G. B. *Org. Biomol. Chem.* **2010**, *8*, 1340−1343.
(26) Horner, J. H.; Lal, M.; Newcomb, M. *Org. Lett.* **2006**, *8*, 5497−5500.
(27) Horner, J. H.; Bagnol, L.; Newcomb, M. *J. Am. Chem. Soc.* **2004**, *126*, 14979−14987.
(28) Horner, J. H.; Taxil, E.; Newcomb, M. *J. Am. Chem. Soc.* **2002**, *124*, 5402−5410.
(29) Newcomb, M.; Miranda, N.; Sannigrahi, M.; Huang, X.; Crich, D. *J. Am. Chem. Soc.* **2001**, *123*, 6445−6446.
(30) Horner, J. H.; Newcomb, M. *J. Am. Chem. Soc.* **2001**, *123*, 4364−4365.
(31) Steenken, S.; Jovanovic, S. V. *J. Am. Chem. Soc.* **1997**, *119*, 617−618.
(32) Psciuk, B. T.; Lord, R. L.; Munk, B. H.; Schlegel, H. B. *J. Chem. Theory Comput.* **2012**, *8*, 5107−5123.
(33) Zheng, L.; Greenberg, M. M. *J. Am. Chem. Soc.* **2017**, *139*, 17751−17754.
(34) See the Supporting Information.
(35) Zhu, Q.; Delaney, M. O.; Greenberg, M. M. *Bioorg. Med. Chem. Lett.* **2001**, *11*, 1105−1108.
(36) Meggers, E.; Michel-Beyerle, M. E.; Giese, B. *J. Am. Chem. Soc.* **1998**, *120*, 12950−12955.
(37) Saito, I.; Nakanura, T.; Nakatani, K.; Yoshioka, Y.; Yamaguchi, K.; Sugiyama, H. *J. Am. Chem. Soc.* **1998**, *120*, 12686−12687.
(38) Hall, D. B.; Holmlin, R. E.; Barton, J. K. *Nature* **1996**, *382*, 731−735.
(39) Rogstad, D. K.; Heo, J.; Vaidehi, N.; Goddard, W. A.; Burdzy, A.; Sowers, L. C. *Biochemistry* **2004**, *43*, 5688−5697.
(40) Masaoka, A.; Matsubara, M.; Hasegawa, R.; Tanaka, T.; Kurisu, S.; Terato, H.; Ohyama, Y.; Karino, N.; Matsuda, A.; Ide, H. *Biochemistry* **2003**, *42*, 5003−5012.
(41) Zheng, L.; Greenberg, M. M. *J. Am. Chem. Soc.* **2018**, *140*, 6400−6407.
(42) Zheng, L.; Griesser, M.; Pratt, D. A.; Greenberg, M. M. *J. Org. Chem.* **2017**, *82*, 3571−3580.
(43) Fujimoto, J.; Tran, L.; Sowers, L. C. *Chem. Res. Toxicol.* **1997**, *10*, 1254−1258.
(44) Morningstar, M. L.; Kreutzer, D. A.; Essigmann, J. M. *Chem. Res. Toxicol.* **1997**, *10*, 1345−1350.
(45) Cadet, J.; Douki, T.; Frelon, S.; Sauvaigo, S.; Pouget, J. P.; Ravanat, J. L. *Free Radical Biol. Med.* **2002**, *33*, 441−449.
(46) Carter, K. N.; Greenberg, M. M. *J. Am. Chem. Soc.* **2003**, *125*, 13376−13378.
(47) Ni, J.; Pomerantz, S. C.; Rozenski, J.; Zhang, Y.; McCloskey, J. A. *Anal. Chem.* **1996**, *68*, 1989−1999.
(48) Chowdhury, G.; Guengerich, F. P. *Angew. Chem., Int. Ed.* **2008**, *47*, 381−384.
(49) Chowdhury, G.; Guengerich, F. P. *Chem. Res. Toxicol.* **2009**, *22*, 1310−1319.
(50) Wang, Y. *Chem. Res. Toxicol.* **2002**, *15*, 671−676.
(51) Chen, S. B.; Li, Y. M.; Luo, S. Z.; Zhao, G.; Tan, B.; Zhao, Y. F. *Phosphorus, Sulfur Silicon Relat. Elem.* **2000**, *164*, 277−291.
(52) Gasper, S. M.; Schuster, G. B. *J. Am. Chem. Soc.* **1997**, *119*, 12762−12771.

DOI: 10.1021/jacs.8b05484
J. Am. Chem. Soc. XXXX, XXX, XXX−XXX